# Electronic Supplementary Material

# Gate-controlled supercurrent effect in dry-etched Dayem bridges of non-centrosymmetric niobium rhenium

Jennifer Koch[1], Carla Cirillo[2], Sebastiano Battisti[3], Leon Ruf[1], Zahra Makhdoumi Kakhaki[4], Alessandro Paghi[3], Armen Gulian[5], Serafim Teknowijoyo[5], Giorgio De Simoni[3], Francesco Giazotto[3], Carmine Attanasio[4], Elke Scheer[1] (✉), and Angelo Di Bernardo[1,4] (✉)

[1] *Department of Physics, University of Konstanz, Universitätsstraße 10, 78464 Konstanz, Germany*
[2] *CNR-Spin, c/o Università degli Studi di Salerno, via Giovanni Paolo II 132, 84084 Fisciano (SA), Italy*
[3] *NEST, Istituto Nanoscienze-CNR and Scuola Normale Superiore, Piazza San Silvestro 12, 56127 Pisa,, Italy*
[4] *Dipartimento di Fisica "E. R. Caianiello", Università degli Studi di Salerno, Via Giovanni Paolo II 132, 84084 Fisciano (SA), Italy*
[5] *Advanced Physics Laboratory, Institute for Quantum Studies, Chapman University, Burtonsville, MD 20866, USA*

Supporting information to https://doi.org/10.1007/s12274-024-6576-7

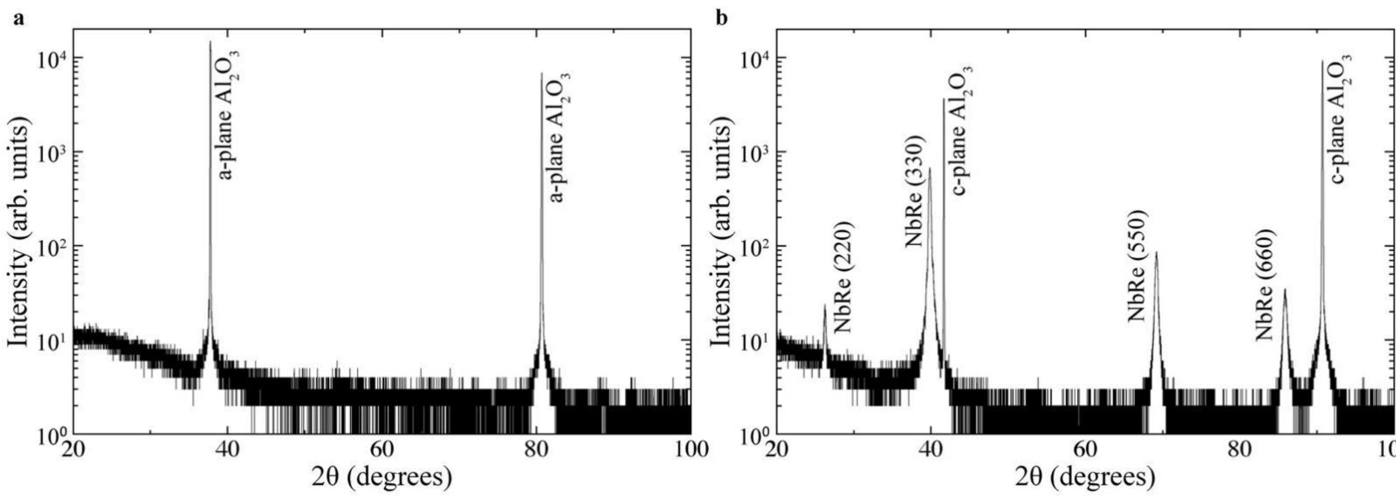


**Figure S1** High-angle X-ray diffraction patterns of NbRe thin films. (a) 2theta-omega scan of a 20-nm-thick $Nb_{0.18}Re_{0.82}$ thin film and (b) same scan for a 30-nm-thick $Nb_{0.10}Re_{0.90}$ thin film.

Address correspondence to E. Scheer, elke.scheer@uni-konstanz.de; A. Di Bernardo, angelo.dibernardo@uni-konstanz.de

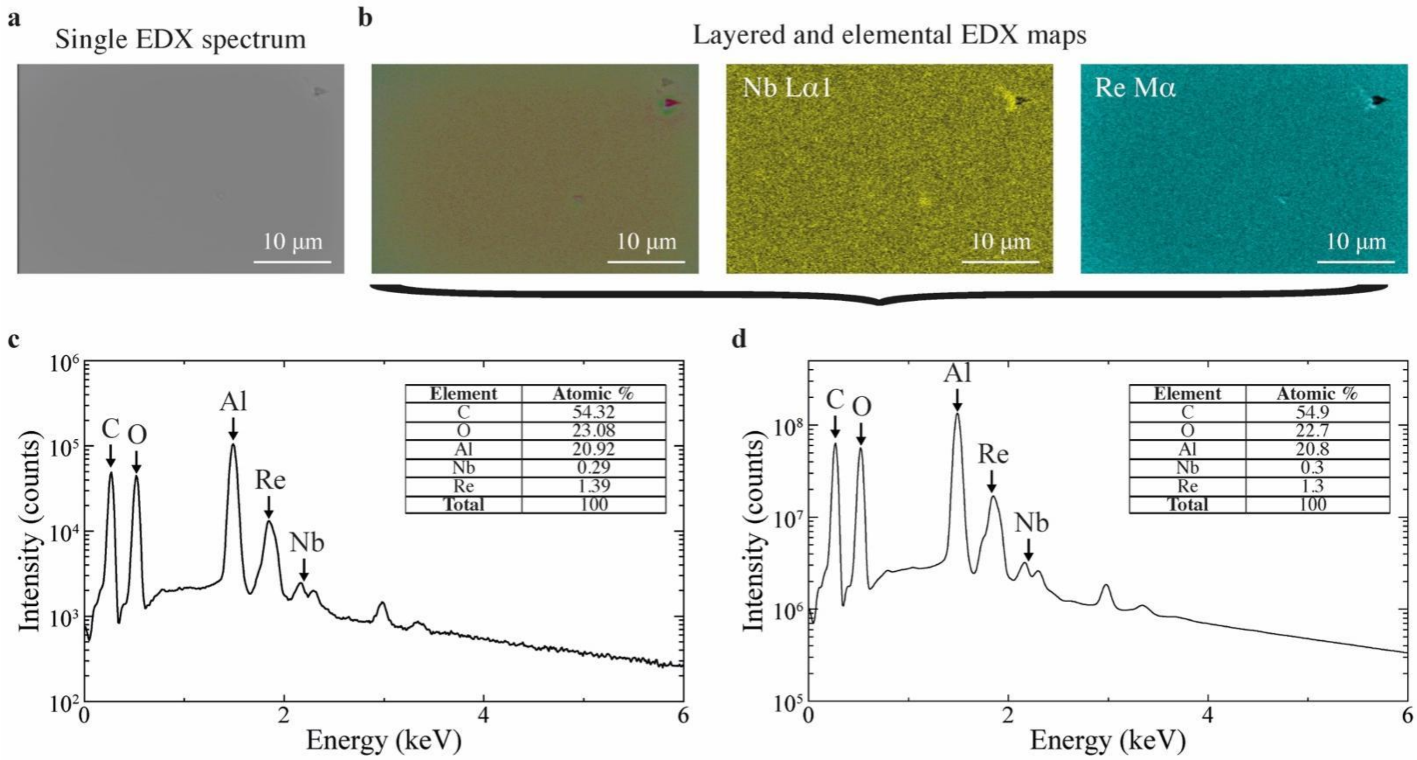


**Figure S2** Energy-dispersive X-ray (EDX) analysis of a $Nb_{0.18}Re_{0.82}$ thin film. (a) Scanning electron microscope image of a sample area on which the EDX spectrum in (c) has been measured with an acceleration voltage of 10 kV. (b) EDX map measured at the same acceleration voltage of 10 kV on the same area as in (a) with all the elements layered (left panel) and element-specific for Nb (middle panel) and Re (right panel). (d) Sum of the EDX spectra composing the map shown in (b). The atomic concentrations of the single elements estimated from the spectra in (c) and (d) are shown in the tables of the corresponding panels.

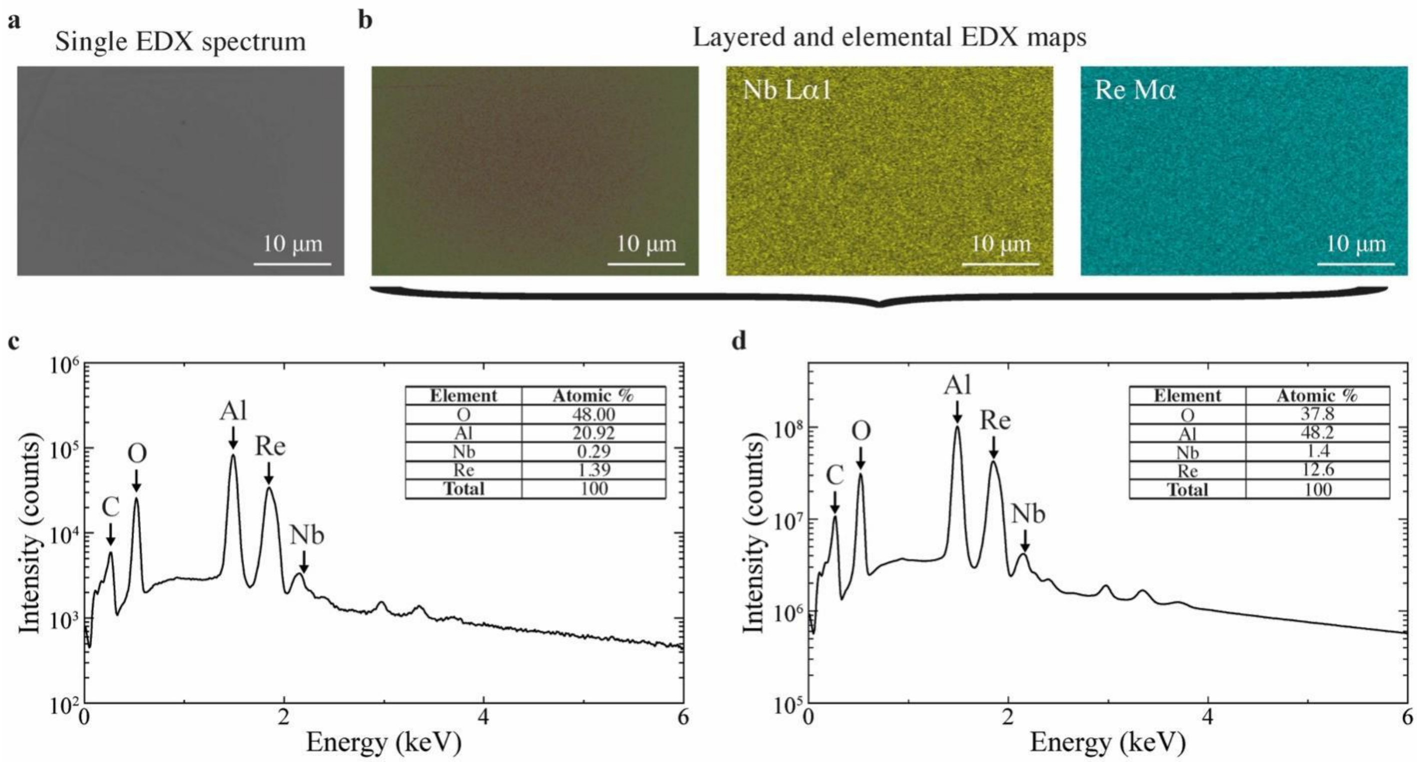


**Figure S3** Energy-dispersive X-ray (EDX) analysis of a $Nb_{0.10}Re_{0.90}$ thin film. (a) Scanning electron microscope image of a sample area on which the EDX spectrum in (c) has been measured with an acceleration voltage of 10 kV. (b) EDX map measured at the same acceleration voltage of 10 kV on the same area as in (a) with all the elements layered (left panel) and element-specific for Nb (middle panel) and Re (right panel). (d) Sum of the EDX spectra composing the map shown in (b). The atomic concentrations of the single elements estimated from the spectra in (c) and (d) are shown in the tables of the corresponding panels.

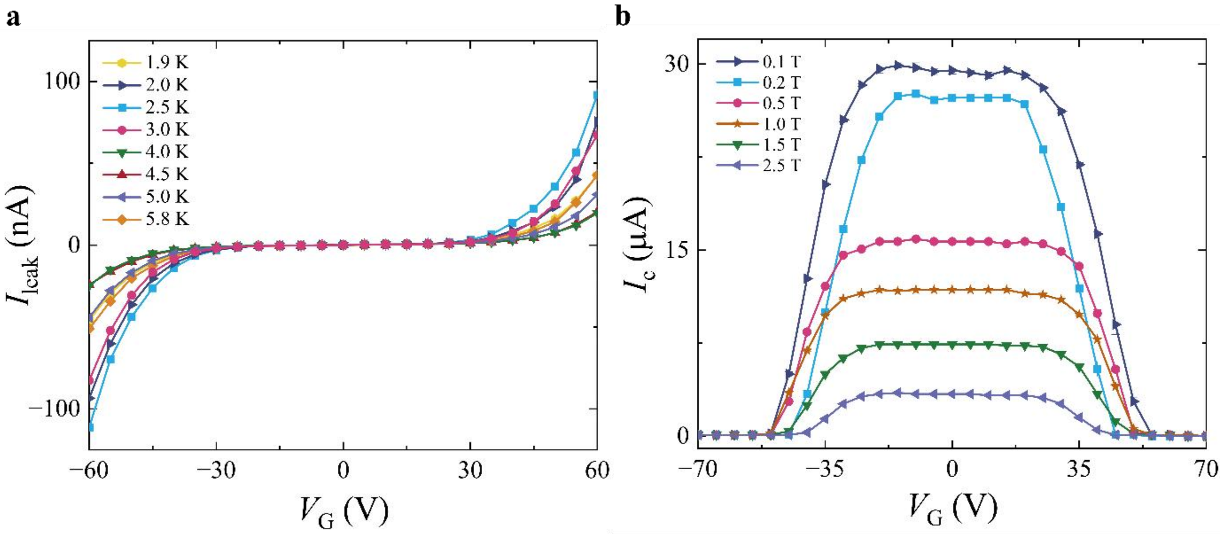


**Figure S4** Gate-controlled supercurrent effect and its magnetic field dependence for NbRe device D1. (a) Leakage current versus gate voltage, $I_{leak}(V_G)$, curves for device D1 measured at different temperature $T$s (specified in the panel legend). (b) Critical current versus gate voltage, $I_c(V_G)$, curves measured for the same device at different applied out-of-plane magnetic fields (specified in the panel legend).

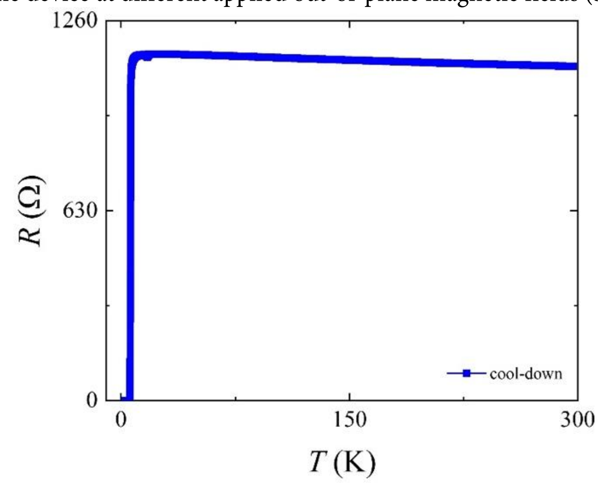


**Figure S5** Resistance versus temperature $R(T)$ curve of device D1. $R(T)$ curve measured in cooling from 297 K down to 2.8 K for a $Nb_{0.18}Re_{0.82}$ thin film showing a residual resistivity ratio below 1.

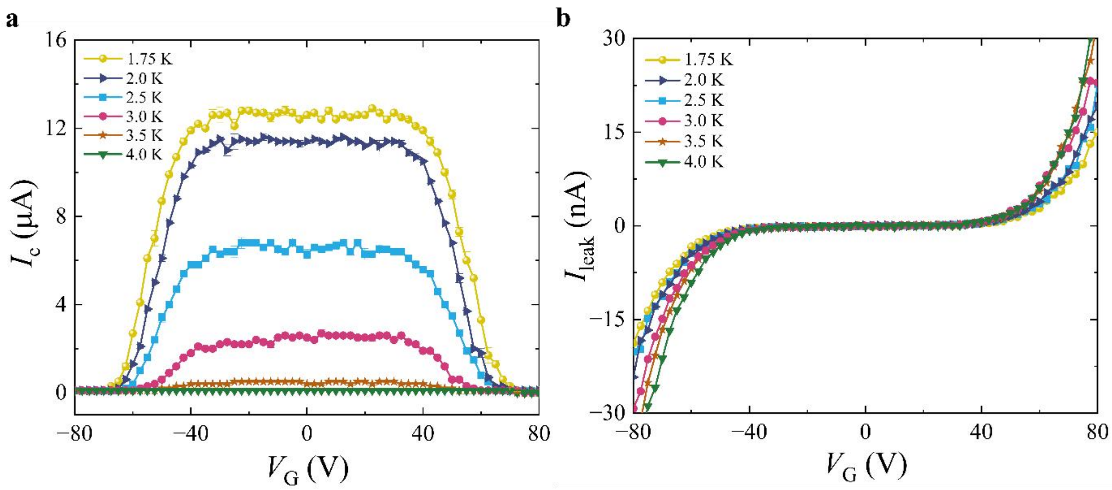


**Figure S6** Gate-controlled supercurrent effect in NbRe device D2. (a) $I_c(V_G)$ curves measured for device D2 at different $T$s (specified in the panel legend) with corresponding $I_{leak}(V_G)$ curves at the same $T$s in (b).

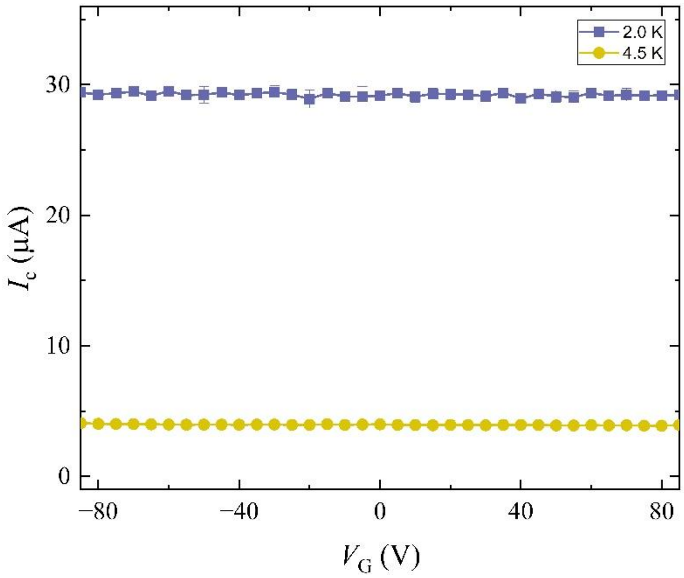


**Figure S7** Absence of gate-controlled supercurrent effect in NbRe device D6. $I_c(V_G)$ curves measured for device D6 at different $T$s (specified in the panel legend) showing no suppression in $I_c$ under an applied $V_G$ up to 80 V.

**Table S1** Parameters for all NbRe Dayem bridge devices tested. The Table reports, for each device, its geometric parameters (i.e., gate-to-channel distance, width, and length of the Dayem bridge), transport parameters (e.g., normal-state resistance $R_N$ and the $I_c$ measured at $V_G = 0$) and the gas mixture used for etching. Devices made from 20-nm-thick NbRe thin films with composition $Nb_{0.18}Re_{0.82}$ are highlighted in blue, whilst those made from 30-nm-thick $Nb_{0.10}Re_{0.90}$ are highlighted in red. As explained in the main text, GCS is only observed for devices from D1 to D3 etched in an $Ar/Cl_2$ mixture from disordered $Nb_{0.18}Re_{0.82}$ thin films.

| Device name | Gate-to-channel-distance $d_g$ [nm] | Width of the wire $w$ [nm] | Length of the wire $l$ [nm] | $R_N$ at 10 K [Ω] | $I_c$ at $V_G = 0$ V [μA] | Etching gas mixture |
|---|---|---|---|---|---|---|
| D1 | 312 | 64 | 219 | 1144 | 27.2 (2 K) | $Ar + Cl_2$ |
| D2 | 291 | 61 | 217 | 830 | 11.4 (2 K) | $Ar + Cl_2$ |
| D3 | 321 | 56 | 214 | 1261 | 14.5 (2 K) | $Ar + Cl_2$ |
| D4 | 91 | 71 | 207 | 928 | 53 (2.37 K)/58.6 (1.6 K) | Ar |
| D5 | 97 | 60 | 183 | 741 | 67 (1.65 K) | Ar |
| D6 | ≈ 125 | ≈ 67 | ≈ 218 | 1141 | 29.2 (2 K) | $Ar + SF_6$ |
| D7 | ≈ 125 | ≈ 67 | ≈ 218 | 1755 | 0.9 (3.1 K) | $Ar+SF_6$ |
| D8 | ≈ 50 | 85 | 180 | 2276 | 109 (3.0 K) | $Ar + CF_4 + O_2$ (with Al mask) |
| D9 | ≈ 50 | 70 | 175 | 2301 | 101 (3.0 K) | $Ar + CF_4 + O_2$ (with Al mask) |
| D10 | ≈ 50 | ≈ 200 | 220 | 169.5 | 350 (4.0 K) | $Ar + Cl_2$ |